

Zero-Field Splitting Parameters of Cr^{3+} in Lithium Potassium Sulphate at Orthorhombic Symmetry Site

S. PANDEY AND R. KRIPAL*

EPR Laboratory, Department of Physics, University of Allahabad, Allahabad 211002, India

(Received April 28, 2011; in final form October 25, 2012)

The superposition model is used to investigate the crystal field parameters, B_{kq} of Cr^{3+} in lithium potassium sulphate. The zero field splitting parameters D and E are then determined using microscopic spin Hamiltonian theory and compared with the experimental values obtained by electron paramagnetic resonance. Both zero field splitting parameters D and E evaluated theoretically are in good agreement with the experimental values. The results suggest that the Cr^{3+} ion occupies substitutional K^+ site in lithium potassium sulphate.

DOI: 10.12693/APhysPolA.123.101

PACS: 76.30.-v, 76.30.Fc

1. Introduction

The superposition model was introduced to separate the physical and geometrical information existing in rare-earth ion crystal field parameters [1]. Its application to the spin Hamiltonian (SH) parameters of d^5 ion ground state was also developed [2]. Some success in applying this model to the orbit lattice interaction was achieved. The usual problem in applying this model lies in finding the positions of various ligands. Hence the link between the model and the theories of local distortion in crystals is of considerable interest.

Cr^{3+} ion in an octahedral environment is a very attractive system, which is continuously receiving considerable attention of many research groups. Very specific energy level structure of Cr^{3+} ion with spin-quartet and spin-doublet levels gives an opportunity to reveal dynamic and static properties of Cr^{3+} impurity centers [3, 4].

The superposition model [5, 6] has been successfully applied to gain very detailed information on the lattice site and crystalline environment of Cr^{3+} ion in crystals [7, 8]. This model was successfully applied to Cr^{3+} ion doped RbCdF_3 [9] and ammonium dihydrogen phosphate [10].

Theoretical studies on the spin Hamiltonian parameters have become the subject of a considerable number of works [11–15]. Various mechanisms have been suggested to contribute to ground-state splitting of the magnetic ions interacting with the lattice [16]. The mostly used procedure treats cubic field and the diagonal part of free-ion Hamiltonian as unperturbed Hamiltonian, leaving the perturbations as the spin-orbit coupling, the low-symmetry field, and the off-diagonal part of free-ion Hamiltonian. This procedure was proposed by Macfarlane for F -state ions that gives better results [9].

Electron paramagnetic resonance (EPR) studies of Cr^{3+} impurities in ammonium lithium sulphate (ALS) and lithium potassium sulphate (LPS) single crystals,

which belong to the materials with the general formula $M'M''\text{BX}_4$ ($M' = \text{Li}$; $M'' = \text{Na}, \text{K}, \text{Rb}, \text{Cs}, \text{NH}_4, \text{N}_2\text{H}_5$; $\text{BX}_4 = \text{BeF}_4, \text{SO}_4, \text{SeO}_4$), have been reported [17, 18]. There are three possibilities for the site of Cr^{3+} centre in LPS crystal, namely substitution at K^+ site, substitution at Li^+ site and interstitial. It is interesting to determine the site of this impurity. It was found that Cr^{3+} enters the lattice substitutionally at K^+ site [17]. In this paper, we present the calculated zero field splitting parameters (ZFSPs), using crystal field parameters from superposition model [16] for the Cr^{3+} ion present at substitutional K^+ site in LPS. The result derived from this model is consistent with the experimental observation.

2. Crystal structure

The crystal structure of LiKSO_4 was determined by Karppinen et al. [19]. The structure is hexagonal, space group $P6_3$ with $Z = 2$. The unit cell dimensions are $a = 0.51452$ nm and $c = 0.86343$ nm. The structure consists of Li^+ and SO_4^{2-} ions lying on threefold axes and K^+ ions lying on sixfold axes. The Li^+ ion has a tetrahedral coordination with Li–O distances in the range 0.1909–0.1923 nm. The K^+ ion is surrounded by nine O atoms of sulphate at distances 0.2840–0.2989 nm. The arrangement of O ligands may be described as a distorted octahedron with additional O atoms outside three of its edges (Fig. 1a).

3. Theoretical investigation

The experimental results for the resonance field of Cr^{3+} in LPS single crystals can be analyzed with the usual spin Hamiltonian [20]:

$$\mathcal{H} = \mu_B B g S + D \left[S_z^2 - \frac{S(S+1)}{3} \right] + E(S_x^2 - S_y^2), \quad (1)$$

where μ_B is the Bohr magneton, g is spectroscopic splitting factor, D is axial zero field splitting parameter and E is rhombic zero field splitting parameter. In the above equation, first term represents the electron Zeeman interaction, second term represents the axial zero field splitting and third term represents the rhombic zero field splitting.

*corresponding author; e-mail: ram_kripal2001@rediffmail.com

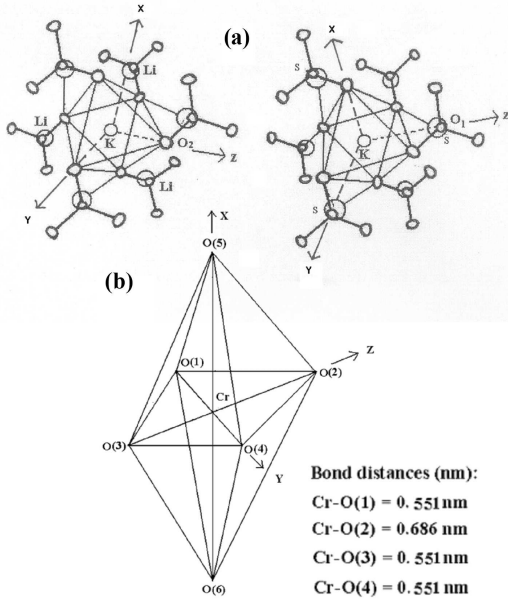


Fig. 1. (a) The environment of K⁺ viewed along the *c* axis (by the courtesy of M. Karppinen et al. [17]). (b) Coordination around Cr³⁺ in LPS.

The crystal field Hamiltonian can be written as [21]:

$$\mathcal{H} = \sum_{k,q} B_{kq} C_q^{(k)}, \quad (2)$$

where B_{kq} are the crystal-field parameters and $C_q^{(k)}$ are the Wybourne spherical tensor operators. For the orthorhombic symmetry of the crystal field, $B_{kq} \neq 0$ only with $k = 2, 4, q = 0, 2, 4$. In the present study, the crystal-field parameters, B_{kq} are calculated using superposition model [22–27]. Considering the transformation properties of the Stevens operators O_k^q , the relations between the arbitrary symmetry spin Hamiltonian parameters and crystal field parameters in the Stevens notation B_k^q were derived in various axis systems [28]. Using consistent convention prevailing in the recent literature we have the following relations between the conventional ZFS parameters D and E and crystal field parameters B_k^q :

$$D = 3B_2^0, \quad E = B_2^2. \quad (3)$$

Taking these relations and the idea that the ratio E/D for an orthorhombic symmetry Hamiltonian can always be limited to the range $(0, \pm 1/3)$, the conventional D and E are calculated by obtaining B_k^q from B_{kq} (crystal field parameters in the Wybourne notation) [29], where B_{kq} are determined from the expressions given in Appendix A.

By considering the covalency effect via the average covalency parameter N , the Racah parameters B, C and the spin-orbit coupling parameter, ξ_d can be expressed in terms of N as [21] $B = N^4 B_0, C = N^4 C_0; \xi_d = N^2 \xi_d^0$, where B_0 and C_0 , and ξ_d^0 are the free ion Racah and the spin-orbit coupling parameters, respectively [21] ($B_0 = 918 \text{ cm}^{-1}, C_0 = 3430 \text{ cm}^{-1}, \xi_d^0 = 276 \text{ cm}^{-1}$ [20]). With

$B = 697 \text{ cm}^{-1}$ and $C = 3247 \text{ cm}^{-1}$ obtained from optical absorption [18], $N^2 = (\sqrt{B/B_0} + \sqrt{C/C_0})/2$ [30] yields $N = 0.92$. This value of N is used to calculate ξ_d from ξ_d^0 . B, C, ξ_d together with spin-spin interaction, spin-orbit interaction parameters and crystal field parameters B_{kq} are used to calculate the optical spectra of Cr³⁺: LPS crystal with the help of CFA program (discussed later).

3.1. Superposition model

The superposition model has been shown to be quite successful in explaining the crystal-field splitting of the $4f^n$ ions [31] and recently of some $3d^n$ ions [6, 32, 33]. This model expresses the crystal field parameters as [5, 16]:

$$B_{kq} = \sum_j \bar{A}_k(R_j) K_{kq}(\theta_j, \phi_j), \quad (4)$$

where R_j are the distances between the paramagnetic ion and the ligand ion j , R_0 is the reference distance, normally chosen near a value of the R_j 's. θ_j are the bond angles in a chosen axis system (preferably symmetry adopted axis system (SAAS)) [5, 22]. Summation is taken over all the nearest neighbour ligands. The coordination factors $K_{kq}(\theta_j, \phi_j)$ are the explicit functions of angular positions of ligands [16, 22, 23]. The parameter $\bar{A}_k(R_j)$ is given by [16]:

$$\bar{A}_k(R_j) = \bar{A}_k(R_0) (R_0/R_j)^{t_k}, \quad (5)$$

where $\bar{A}_k(R_0)$ is the intrinsic parameter for a given ion host system; t_k is power law exponent.

For $3d^N$ ions in the 6-fold cubic coordination $\bar{A}_4(R_0)$ can be found from the relation [34]: $\bar{A}_4(R_0) = (3/4)Dq$. As $\bar{A}_4(R_0)$ is independent of the coordination [24], we have used above relation to determine $\bar{A}_4(R_0)$ in our calculation. Also, $\bar{A}_2(R_0) = 8\bar{A}_4(R_0)$ [9, 32]. Using $Dq = 2050 \text{ cm}^{-1}$ [18], we get $\bar{A}_4(R_0) = 1537.5 \text{ cm}^{-1}$ and $\bar{A}_2(R_0) = 12300 \text{ cm}^{-1}$. The following values of the superposition-model parameters and the metal-ligand bond distances (Fig. 1b) are adopted: $t_2 = 4, t_4 = 6$ [9]; $t_2 = 8, t_4 = 9; R_1, R_1', R_2, R_2'; \theta_1, \theta_1', \theta_2, \theta_2'; \phi_1, \phi_1', \phi_2$ and ϕ_2' are 0.551 nm, 0.551 nm, 0.551 nm, 0.686 nm; 84.39°, 84.39°, 84.39°, 83.63°; 63.43°, 26.57°, -45° and 49.48°, respectively.

4. Result and discussion

First, assuming interstitial site of Cr³⁺ at the point between O(1)–O(2) bond the origin was shifted at this point. The bond distances of different ligands, R_j and the corresponding angle θ_j were determined and are given in Table I. When R_0 is taken as the average of R_j [13], i.e. $R_0 = 0.511 \text{ nm}, t_2 = 4$ and $t_4 = 6$, we obtain different crystal field parameters resulting D and E to be 11241.7 cm^{-1} and 21586.8 cm^{-1} , respectively, which are inconsistent with the experimental values. Then we have calculated D and E taking the lowest value of the metal-oxygen distances as R_0 [35] i.e. $R_0 = 0.439 \text{ nm}, t_2 = 4$ and $t_4 = 6$, which come out to be -10273.4 cm^{-1} and 1622.1 cm^{-1} , respectively. These are also larger than

the experimental values. Taking $R_0 = 0.187$ nm, sum of ionic radii of O^{2-} (0.132 nm) and Cr^{3+} (0.055 nm), $t_2 = 4$ and $t_4 = 6$, we obtain D and E as 136.1 cm^{-1} and 439.8 cm^{-1} , respectively, which are also larger than the experimental values. Thus interstitial site for Cr^{3+} in LPS seems to be inappropriate. Next to see the substitution at Li^+ site, the origin of Cr^{3+} was shifted at the Li^+ ion.

TABLE I

Metal-oxygen bond distances R_j and coordination angles θ_j in Cr^{3+} ion doped LPS single crystals (when the Cr^{3+} ion is assumed at point between of O(1)-O(2) bond).

Metal-oxygen	Bond distance R_j [nm]	Angle θ_j [degree]	Angle ϕ_j [degree]
Cr-O(1)	0.514	83.57	49.47
Cr-O(3)	0.481	83.57	49.47
Cr-O(4)	0.439	83.57	49.48
Cr-O(2)	0.611	83.45	49.48

The bond distances of different ligands, R_j and the angle θ_j were calculated and are given in Table II. Taking R_0 as the average of R_j [13], i.e. $R_0 = 0.423$ nm, $t_2 = 4$ and $t_4 = 6$, we obtain D and E to be -1108537 cm^{-1} and 599184 cm^{-1} , respectively, which are inconsistent with the experimental values. We have then calculated D and E taking the lowest value of the metal-oxygen distances as R_0 [35] i.e. $R_0 = 0.191$ nm, $t_2 = 4$ and $t_4 = 6$, that come out to be -45613 cm^{-1} and 24655 cm^{-1} , respectively. These are also inconsistent with the experimental values. Taking $R_0 = 0.187$ nm (sum of ionic radii of O^{2-} and Cr^{3+}), $t_2 = 4$ and $t_4 = 6$, we obtain D and E as -41987 cm^{-1} and 22694 cm^{-1} , respectively, which are also larger than the experimental values. Thus the above results suggest that the Li^+ site is not appropriate for substitution of Cr^{3+} .

TABLE II

Metal-oxygen bond distances R_j and coordination angles θ_j in Cr^{3+} ion doped LPS single crystals (when the Cr^{3+} ion is assumed at Li^+ site).

Metal-oxygen	Bond distance R_j [nm]	Angle θ_j [degree]	Angle ϕ_j [degree]
Cr-O(1)	0.191	83.35	0
Cr-O(3)	0.549	87.69	45
Cr-O(4)	0.549	87.69	0
Cr-O(2)	0.407	83.74	-87.02

The origin of Cr^{3+} was then shifted at the K^+ ion site and bond distances of different ligands, R_j and angle θ_j were determined as shown in Table III. Taking R_0 as the average of R_j [13], i.e. $R_0 = 0.585$ nm, $t_2 = 4$ and $t_4 = 6$, we obtain different crystal field parameters resulting D and E to be -24528.9 cm^{-1} and -1591.4 cm^{-1} , respectively, which is larger than the experimental values. We have then calculated D and E taking above R_0 (0.585 nm) and $t_2 = 8$ and $t_4 = 9$, which are -33822.4 cm^{-1} and -11051.4 cm^{-1} , respectively. These

are also larger than the experimental values. We have also calculated D and E taking the lowest value of the metal-oxygen distances as R_0 [35] i.e. $R_0 = 0.551$ nm, $t_2 = 4$ and $t_4 = 6$, which come out to be -19386.5 cm^{-1} and -1257.7 cm^{-1} , respectively. These values are also inconsistent with the experimental values. D and E are also calculated taking above R_0 (0.551) and $t_2 = 8$ and $t_4 = 9$, which are -21127.5 cm^{-1} and -6903.4 cm^{-1} , respectively. These values also do not match with the experimental values. Taking $R_0 = 0.187$ nm (sum of ionic radii of Cr^{3+} and O^{2-} [36]), $t_2 = 4$ and $t_4 = 6$, we found D and E as -255.4 cm^{-1} and -16.5 cm^{-1} , respectively, which are also not consistent with the experimental values. Taking above R_0 (0.187 nm) and $t_2 = 8$ and $t_4 = 9$, D and E are found as -3.7 cm^{-1} and -1.2 cm^{-1} , respectively. These are also larger than the experimental values. Therefore, we have taken $R_0 = 0.110$ nm, which is slightly lower than the sum of ionic radii of Cr^{3+} and O^{2-} (0.187 nm). This R_0 value together with $t_2 = 4$ and $t_4 = 6$ provides D and E data as -30.6 cm^{-1} and -1.98 cm^{-1} , respectively, which is also inconsistent with the experimental values.

TABLE III

Metal-oxygen bond distances R_j and coordination angles θ_j in Cr^{3+} ion doped LPS single crystals (when Cr^{3+} ion is assumed at K^+ site).

Metal-oxygen	Bond distance R_j [nm]	Angle θ_j [degree]	Angle ϕ_j [degree]
Cr-O(1)	0.551	84.39	63.43
Cr-O(3)	0.551	84.39	26.57
Cr-O(4)	0.551	84.39	-45
Cr-O(2)	0.686	83.63	49.48

Then we have taken $R_0 = 0.110$ nm and $t_2 = 8$, $t_4 = 9$ and obtain D and E as $-525 \times 10^{-4} \text{ cm}^{-1}$ and $-172 \times 10^{-4} \text{ cm}^{-1}$ (Table IV), respectively, which are in reasonable agreement with the experimental values. Therefore, we can say that K^+ site is the better candidate for substitution of Cr^{3+} . In this way, the conclusion drawn on the basis of superposition model supports the experimental result that Cr^{3+} ions take up substitutional K^+ site in the crystal [18]. The effective impurity-ligand distance (or reference bond length) is different as compared to the corresponding metal-ligand distance. This may be due to the difference in charge and ionic radius between the Cr^{3+} and the replaced K^+ in LPS [37]. This may also be due to an off-center displacement of the impurity ion in LPS. The calculations using different models of defect structure considering an off-center displacement of the impurity ion are in progress and the results will be published soon.

The expressions for crystal-field parameters B_{kq} , for the impurity at orthorhombic symmetry site, using Eq. (4) are given [11] in Appendix A. The calculated values of B_{kq} parameters for Cr^{3+} ions at K^+ site ($R_0 = 0.110$ nm) are obtained (in 10^{-4} cm^{-1}) as: $B_{20} = 245.32$, $B_{22} = -455.51$, $B_{40} = -17.86$, $B_{42} = 27.21$,

TABLE IV

Comparison of the ZFS parameters calculated by the superposition model for the Cr^{3+} ion (at K^+ site) in LPS single crystal with experimental values.

	Values of ZFS parameters ($\times 10^{-4} \text{ cm}^{-1}$)		
	$ D $	$ E $	$ E / D $
calculated	525	172	0.32
experimental	549	183	

$B_{44} = 27.08$. These CFPs are non-standard. Using S4/S6 transformation [29], the standard CFPs are obtained (in 10^{-4} cm^{-1}) as: $B_{20} = -350.4$, $B_{22} = -140.2$, $B_{40} = -6.7$, $B_{42} = 71.8$, $B_{44} = -50.9$. B_2^0 and B_2^2 , CFPs in the Stevens notation [30] are found as -0.01752 cm^{-1} and -0.1717 cm^{-1} , respectively. The ZFS parameters D and E are obtained by using $D = 3B_2^0$ and $E = B_2^2$.

The $|D|$ and $|E|$ values thus obtained are given in Table IV. The ratio $|E|/|D|$ comes out to be 0.32, which is standard one. The experimental values are also shown here for comparison. The calculated values of the ZFS

parameters are in reasonable agreement with the values obtained from the experiment [18]. Using above B_{kq} parameters and CFA program [38, 39] the optical spectra of Cr^{3+} doped LPS crystals are calculated. The CFA program allows obtaining the complete energy level scheme for any $3d^N$ ion in a crystal field of arbitrarily low symmetry within the whole basis of $3d^N$ states. The energy levels of the impurity ion are obtained by diagonalization of the complete Hamiltonian within the $3d^N$ basis of states in the intermediate crystal field coupling scheme. The Hamiltonian includes the Coulomb interaction (in terms of the Racah parameters B and C), the Trees correction, the spin-orbit interaction, the crystal field Hamiltonian, the spin-spin interaction and the spin-other-orbit interaction. $B = 697 \text{ cm}^{-1}$, $C = 3247 \text{ cm}^{-1}$; Trees correction, $\alpha = 70 \text{ cm}^{-1}$; spin-orbit interaction parameter, $\xi_d = 254 \text{ cm}^{-1}$; spin-spin interaction parameter, $M_0 = 0.2021 \text{ cm}^{-1}$; spin-spin interaction parameter, $M_2 = 0.0159 \text{ cm}^{-1}$; spin-other-orbit interaction parameter, $M_{00} = 0.2021 \text{ cm}^{-1}$; spin-other-orbit interaction parameter, $M_{22} = 0.0159 \text{ cm}^{-1}$ were used for calculation.

Experimental and theoretical energy values of different transitions in Cr^{3+} doped LPS.

TABLE V

Transition from ${}^4A_{2g}(F)$	Wavenumber [cm^{-1}]	
	observed	calculated
${}^2E_g(G)$	12298 14984	0(16), 0(37), 0(30), 0(23), 204(15), 204(38), 204(22), 204(31), 204(20), 204(33), 478(14), 478(39), 478(32), 478(21), 478(28), 478(25), 478(24), 478(29), 812(40), 812(13), 812(36), 812(17), 812(17), 812(36), 812(18), 812(35), 812(27), 812(26), 10003(9), 10003(4), 10108(5), 10108(8), 10108(10), 10108(3), 10354(7), 10354(6), 10354(11), 10354(2), 10354(1), 10354(12), 13391(88), 13391(91), 13391(93), 13391(86), 13391(95), 13391(84), 13391(97), 13391(82) , 13680(90), 13680(89), 13680(87), 13680(92), 13680(85), 13680(94), 13680(83), 13680(96), 13680(98), 13680(81)
${}^2T_{1g}(G)$	16310 16966 18002	15784(46), 15784(41), 15784(43) , 15784(44) 17665(111), 17665(108), 17665(106), 17665(113), 17665(115), 17665(104), 17665(117), 17665(102), 17665(119), 17665(100) 17782(58), 17782(65), 17782(60), 17782(63), 17865(110), 17865(109), 17865(107), 17865(112), 17865(105), 17865(114), 17865(103), 17865(116), 17865(118), 17865(101), 17865(120), 17865(99)
${}^4T_{2g}(F)$	20504	17961(57), 17961(66), 17961(64), 17961(59), 17961(61), 17961(62)
${}^4T_{1g}(F)$	25026 27732 28957	26872(74), 26872(73), 26872(71), 26872(76) 26872(69), 26872(78), 26872(67) , 26872(80) 27052(75), 27052(72), 27052(70), 27052(77), 27052(68), 27052(79)
${}^2A_{1g}(G)$	32927	42601(51), 42601(52), 42601(54), 42601(49)
${}^2T_{2g}(H)$	36551	42601(47), 42601(56), 42742(53), 42742(50), 42742(48), 42742(55)

The calculated energy values are given in Table V along with the experimental ones for comparison. There is a reasonable agreement between these two. Thus, we confirm that the Cr^{3+} ion enters the LPS lattice substitutionally at K^+ site and the calculated parameters (B_{kq} , D and E) are convincing. The calculated ZFS parameters using superposition model may be used to identify the site of the Cr^{3+} centre.

5. Conclusion

The EPR ZFS parameters have been investigated using the superposition model and microscopic spin Hamiltonian theory. The experimental ZFS parameters obtained for the Cr^{3+} ion in LPS single crystal are in reasonable agreement with the calculated ZFS parameters at the substitutional K^+ site. The calculated optical spectra are in reasonable agreement with the experimental ones. We confirm that the Cr^{3+} ion occupies substitutional K^+

site in LPS. The results support the inference drawn from experimental data.

Appendix A

Relations for the crystal-field parameters derived within the superposition model for the Cr^{3+} ion positioned at the K^+ site in LPS

$$B_{20} = \overline{A}_2(R_0) [(R_0/R_1)^{t_2} (3 \cos^2 \theta_1 - 1) + (R_0/R_1')^{t_2} (3 \cos^2 \theta_1' - 1) + (R_0/R_2)^{t_2} (3 \cos^2 \theta_2 - 1) + (R_0/R_2')^{t_2} (3 \cos^2 \theta_2' - 1)], \quad (A1)$$

$$B_{22} = \sqrt{6} \overline{A}_2(R_0) [(R_0/R_1)^{t_2} \sin^2 \theta_1 \cos(2\phi_1) + (R_0/R_1')^{t_2} \sin^2 \theta_1' \cos(2\phi_1') + (R_0/R_2)^{t_2} \sin^2 \theta_2 \cos(2\phi_2) + (R_0/R_2')^{t_2} \sin^2 \theta_2' \cos(2\phi_2')]/2, \quad (A2)$$

$$B_{40} = \overline{A}_4(R_0) [(R_0/R_1)^{t_4} (35 \cos^4 \theta_1 - 30 \cos^2 \theta_1 + 3) + (R_0/R_1')^{t_4} (35 \cos^4 \theta_1' - 30 \cos^2 \theta_1' + 3) + (R_0/R_2)^{t_4} (35 \cos^4 \theta_2 - 30 \cos^2 \theta_2 + 3) + (R_0/R_2')^{t_4} (35 \cos^4 \theta_2' - 30 \cos^2 \theta_2' + 3)], \quad (A3)$$

$$B_{42} = \sqrt{10} \overline{A}_4(R_0) [(R_0/R_1)^{t_4} \sin^2 \theta_1 (7 \cos^2 \theta_1 - 1) \times \cos(2\phi_1) + (R_0/R_1')^{t_4} \sin^2 \theta_1' (7 \cos^2 \theta_1' - 1) \cos(2\phi_1') + (R_0/R_2)^{t_4} \sin^2 \theta_2 (7 \cos^2 \theta_2 - 1) \cos(2\phi_2) + (R_0/R_2')^{t_4} \sin^2 \theta_2' (7 \cos^2 \theta_2' - 1) \cos(2\phi_2')], \quad (A4)$$

$$B_{44} = \sqrt{70} \overline{A}_4(R_0) [(R_0/R_1)^{t_4} \sin^4 \theta_1 \cos(4\phi_1) + (R_0/R_1')^{t_4} \sin^4 \theta_1' \cos(4\phi_1') + (R_0/R_2)^{t_4} \sin^4 \theta_2 \cos(4\phi_2) + (R_0/R_2')^{t_4} \sin^4 \theta_2' \cos(4\phi_2')]/2. \quad (A5)$$

Acknowledgments

The authors are thankful to Prof. C. Rudowicz, Molecular Spectroscopy Group, Szczecin University of Technology, Poland for providing CFA program to calculate optical spectra.

References

- [1] M.I. Bradbury, *Chem. Phys. Lett.* **1**, 44 (1967).
- [2] D.J. Newman, *J. Phys. C, Solid State Phys.* **10**, L315 (1977).
- [3] A.N. Medina, A.C. Bento, M.L. Baesso, F.G. Gandra, T. Catunda, A. Cassanho, *J. Phys., Condens. Matter* **13**, 8435 (2001).
- [4] O.S. Wenger, R. Valiente, H.U. Gudel, *J. Chem. Phys.* **115**, 3819 (2001).
- [5] D.J. Newman, B. Ng, *Rep. Prog. Phys.* **52**, 699 (1989).
- [6] Y.Y. Yeung, D.J. Newman, *Phys. Rev. B* **34**, 2258 (1986).
- [7] C. Rudowicz, *Phys. Rev. B* **37**, 27 (1988).
- [8] W.C. Zheng, *Phys. Status Solidi B* **143**, 217 (1987).
- [9] Z.Y. Yang, *J. Phys., Condens. Matter* **12**, 4091 (2000).
- [10] R. Kripal, S. Pandey, *Spectrochim. Acta A* **76**, 62 (2010).
- [11] K.T. Han, J. Kim, *J. Phys., Condens. Matter* **8**, 6759 (1996).
- [12] V.K. Jain, V. Kapoor, *J. Phys. Chem. Solids* **53**, 1171 (1992).
- [13] C. Rudowicz, Y.Y. Zhou, *J. Magn. Magn. Mater.* **111**, 153 (1992).
- [14] M.G. Brik, C.N. Avram, N.M. Avram, *Physica B* **384**, 78 (2006).
- [15] K.A. Muller, W. Berlinger, *J. Phys. C., Solid State Phys.* **16**, 6861 (1983).
- [16] W.L. Yu, M.G. Zhao, *Phys. Rev. B* **37**, 9254 (1988).
- [17] R. Kripal, H. Govind, *Physica B* **403**, 3345 (2008).
- [18] R. Kripal, I. Mishra, *Mater. Chem. Phys.* **119**, 230 (2010).
- [19] M. Karppinen, J.-O. Lundgren, R. Liminga, *Acta Crystallogr. C* **39**, 34 (1983).
- [20] A. Abragam, B. Bleaney, *Electron Paramagnetic Resonance of Transition Ions*, Clarendon Press, Oxford 1970.
- [21] T.H. Yeom, S.H. Choh, M.L. Du, M.S. Jang, *Phys. Rev. B* **55**, 3415 (1996).
- [22] M. Andrut, M. Wildner, C. Rudowicz, in: *Spectroscopic Methods in Mineralogy, EMU Notes in Mineralogy*, Vol. 6, Eds. A. Beran, E. Libowitzky, Eötvös University Press, Budapest 2004, Ch. 4, p. 145.
- [23] C. Rudowicz, *J. Phys. C, Solid State Phys.* **20**, 6033 (1987).
- [24] P. Gnutek, Z.Y. Yang, C. Rudowicz, *J. Phys., Condens. Matter* **21**, 455402 (2009).
- [25] Z.Y. Yang, C. Rudowicz, Y.Y. Yeung, *Physica B* **348**, 151 (2004).
- [26] Z.Y. Yang, Y. Hao, C. Rudowicz, Y.Y. Yeung, *J. Phys., Condens. Matter* **16**, 3481 (2004).
- [27] T.H. Yeom, Y.M. Chang, S.H. Choh, C. Rudowicz, *Phys. Status Solidi B* **185**, 409 (1994).
- [28] C. Rudowicz, R. Bramley, *J. Chem. Phys.* **83**, 5192 (1985).
- [29] Y.Y. Yeung, C. Rudowicz, *Computers Chem.* **16**, 207 (1992).
- [30] Q. Wei, *Acta Phys. Pol. A* **118**, 670 (2010).
- [31] D.J. Newman, *Adv. Phys.* **20**, 197 (1970).
- [32] D.J. Newman, D.C. Pryce, W.A. Runciman, *Am. Miner.* **63**, 1278 (1978).
- [33] G.Y. Shen, M.G. Zhao, *Phys. Rev. B* **30**, 3691 (1984).
- [34] *Crystal Field Handbook*, Eds. D.J. Newman, B. Ng, Cambridge University Press, Cambridge 2000.
- [35] Y.Y. Yeung, D.J. Newman, *J. Chem. Phys.* **82**, 3747 (1985).
- [36] R.C. Weast, *CRC Handbook of Chemistry and Physics*, CRC Press, Boca Raton 1989, p. F187.
- [37] S.Y. Wu, H.N. Dong, W.Z. Yan, X.Y. Gao, *Mater. Res. Bull.* **40**, 742 (2005).
- [38] Y.Y. Yeung, C. Rudowicz, *J. Comput. Phys.* **109**, 150 (1993).
- [39] C. Rudowicz, J. Qin, *Phys. Rev. B* **67**, 174420 (2003).